



The reaction of hydopersulfides (RSSH) with S-nitrosothiols (RS-NO) and the biological/physiological implications

Jessica Zarenkiewicz ^{a,1}, Christina Perez-Ternero ^{b,1}, Volga Kojasoy ^{c,1}, Christopher McGinity ^b, Vinayak S. Khodade ^a, Joseph Lin ^d, Dean J. Tantillo ^{c,***}, John P. Toscano ^{a,***}, Adrian J. Hobbs ^{b,**}, Jon M. Fukuto ^{a,e,*}

^a Department of Chemistry, Johns Hopkins University, Baltimore, MD, 21218, USA

^b William Harvey Research Institute, Barts & The London School of Medicine, Queen Mary University of London, Charterhouse Square, London, EC1M 6BQ, UK

^c Department of Chemistry, University of California, Davis, 1 Shields Avenue, Davis, CA, 95616, USA

^d Department of Biology, Sonoma State University, Rohnert Park, CA, 94928, USA

^e Department of Chemistry, Sonoma State University, Rohnert Park, CA, 94928, USA



ARTICLE INFO

Keywords:

S-Nitrosothiols
Hydopersulfides
Hydrogen sulfide
Nitric oxide
Nitroxyl
Transnitrosation
S-Thiolation

ABSTRACT

S-Nitrosothiol (RS-NO) generation/levels have been implicated as being important to numerous physiological and pathophysiological processes. As such, the mechanism(s) of their generation and degradation are important factors in determining their biological activity. Along with the effects on the activity of thiol proteins, RS-NOs have also been reported to be reservoirs or storage forms of nitric oxide (NO). That is, it is hypothesized that NO can be released from RS-NO at opportune times to, for example, regulate vascular tone. However, to date there are few established mechanisms that can account for facile NO release from RS-NO. Recent discovery of the biological formation and prevalence of hydopersulfides (RSSH) and their subsequent reaction with RS-NO species provides a possible route for NO release from RS-NO. Herein, it is found that RSSH is capable of reacting with RS-NO to liberate NO and that the analogous reaction using RSH is not nearly as proficient in generating NO. Moreover, computational results support the prevalence of this reaction over other possible competing processes. Finally, results of biological studies of NO-mediated vasorelaxation are consistent with the idea that RS-NO species can be degraded by RSSH to release NO.

1. Introduction

S-Nitrosothiols (RS-NO) are implicated as playing a role in numerous physiological functions. For example, RS-NO species have been proposed to be storage forms of nitric oxide (NO) capable of being released at opportune times for the control of vascular tone [e.g., [\[1,2\]](#) or intracellular intermediates in the vasorelaxant activity of NO [\[3\]](#). Moreover, aberrant RS-NO generation (e.g., in crucial cysteine-containing proteins) has been proposed to be involved in the etiology of numerous pathophysioses such as in the development of neurodegenerative disease [\[4,5\]](#) or cancer [\[6,7\]](#). Although there is little

doubt that the RS-NO function is prevalent in both small molecules (e.g., S-nitrosoglutathione, GS-NO) and in cysteine-containing proteins, the mechanisms by which they are generated and degraded physiologically remain elusive. Thus, the processes that determine the steady-state levels of RS-NO species are currently unestablished. In the case of possible NO liberation from RS-NO functionalities, many of the proposed mechanisms of RS-NO degradation either do not result in the release of NO or are considered to be physiologically irrelevant [\[8\]](#). Regardless, pathways that establish steady-state RS-NO levels and that can lead to the liberation of NO from RS-NO may have important physiological consequences.

Recent work indicates that hydopersulfides (RSSH) along with other

* Corresponding author. Department of Chemistry, Johns Hopkins University, Baltimore, MD, 21218, USA.

** Corresponding author.

*** Corresponding author.

**** Corresponding author.

E-mail addresses: djtantillo@ucdavis.edu (D.J. Tantillo), jtoscano@jhu.edu (J.P. Toscano), aj.hobbs@qmul.ac.uk (A.J. Hobbs), fukuto@sonoma.edu (J.M. Fukuto).

¹ These authors contributed equally to this work.

Abbreviations

RS-NO	S-nitrosothiol
RSH	thiol
RSSH	hydopersulfide;
RSS-NO	S-nitrosopersulfide;
RSSSR	dialkyltrisulfide;
RSSSSR	dialkyltetrasulfide;
MIMS	membrane inlet mass spectrometry
DTPA	diethylenetriaminepentaacetic acid
GS-NO	S-nitrosoglutathione
PE	phenylephrine;
SNAP	S-nitroso-N-acetyl-penicillamine;
Cys-SSS-Cys	cysteine trisulfide;
L-NAME	N ^G -nitro-L-arginine methylester
ODQ	1H-[1,2,4]oxadiazolo[4,3-a]quinoxalin-1-one
ACh	acetylcholine;
SNP	sodium nitroprusside;
DFT	density functional theory

polysulfur species are prevalent and potentially important biological effectors [for reviews, see [9,10]. One of the prevailing ideas regarding the presence and function of RSSH species is that they can serve a cellular protective role as scavengers of potentially toxic electrophiles and/or deleterious oxidants [e.g., [11]. A rationale for this speculation is that RSSH species are superior reductants and nucleophiles compared to the corresponding thiols and, therefore, capable of facile scavenging of toxic oxidants/electrophiles and/or reversing their effects. An important aspect of this idea is that as an oxidized species, RSSH is more likely generated under cellular oxidizing conditions (i.e., under oxidative stress). This means that a superior reductant/nucleophile, RSSH, can be generated primarily under cellular oxidizing conditions, a situation that may prevent or mitigate oxidation/electrophile-mediated cellular damage. A recent report from our lab also indicates that under purely chemical conditions RSSH reacts readily with R'S-NO species leading to NO liberation and the generation of the corresponding dialkyltetrasulfide (RSSSR) [12]. The proposed mechanism for this observation involves an initial nucleophilic attack of RSSH (likely as the anionic RSS⁻ species) on the electrophilic R'S-NO nitrogen giving, initially, an S-nitrosopersulfide (RSS-NO) intermediate (**Reaction 1**). This reaction is then followed by spontaneous homolysis of the weak S–N bond to give NO and the perthiyl radical species (**Reaction 2**) which in turn will dimerize to the tetrasulfide (**Reactions 3**) [12–14].



Importantly, the homolysis of the intermediate RSS-NO species (**Reaction 2**) is due to the relative stability of the two radical species, NO and RSS[·] [12]. Predictably, S–N homolysis not nearly as facile with R'S-NO species due to the relative instability of R'S[·] (e.g., the R'S[·] is higher in energy compared to RSS[·] and readily reacts with O₂, NO and is a potent oxidant (*vide infra*), while RSS[·] is lower in energy and does not readily react with O₂ or NO and is a weak oxidant).

The chemistry described immediately above is of potential physiological relevance since it represents a mechanism of R'S-NO degradation and therefore could possibly be involved in determining R'S-NO steady-state levels. Moreover, the above R'S-NO degradation chemistry results in the liberation of NO, a process potentially important if indeed R'S-NO species are used as reservoirs and/or storage forms of NO [8]. Considering the possible importance of R'S-NO species to normal physiology as

well as in the etiology of disease and as sources of NO, the chemistry and biological effects of the reaction of RSSH with R'S-NO are further investigated herein.

2. Methods

General Methods: All chemicals were purchased from commercial sources and used as received unless stated otherwise. A Fisher Scientific Accumet AB15 pH-meter was used for pH measurements. GC analysis was performed on an Agilent 8860 equipped with an electron capture detector (ECD) and Restek column (ShinCarbon ST 80/100, 2 m, 1/8" OD).

Synthesis and Characterization: RSSH donor 2-(((3-acetamido-4-methoxy-2-methyl-4-oxobutan-2-yl)disulfane carbonyl)(methyl)amino)-ethan-1-aminium (**1**), GSNO, and *N*-acetylpenicillamine methyl ester were synthesized according to literature procedures and analytical characterization data were consistent with the reported values [15].

Analysis of RSSH/RSH reaction with RS-NO by membrane inlet mass spectrometry (MIMS): MIMS was carried out using a Hiden HPR-40 system containing a 20 mL sample cell and a membrane selective for detecting gases (e.g., NO, N₂O, and H₂S) dissolved in aqueous solution [16,17]. The sample cell was filled with 20 mL of PBS (pH 7.4, 100 mM) containing diethylenetriaminepentaacetic acid (DTPA, 100 μM) and purged with argon for at least 30 min prior to analysis. The sample cell was also wrapped in aluminum foil to prevent photolysis of GSNO. Stock solutions of GSNO were prepared in PBS and RSSH/RSH was prepared in either DMSO or buffer. These stock solutions were purged with nitrogen for 10 min and used shortly after preparation. Aliquots of these solutions were injected into the sample cell using a gastight syringe and masses of interest were monitored with continuous sampling in positive ion mode.

GC Headspace analysis of RSSH/RSH reaction with RS-NO: Thiol stock solutions were prepared in DMSO. In a 15 mL vial sealed with rubber septum, PBS (pH 7.4, 100 mM) containing DTPA (100 μM) was purged with argon for 20 min. These vials were placed in a heated cell block, which was held at 37 °C. The RSSH or thiol and GSNO solutions were added to each vial to obtain 5 mL total volume, and resulting solutions were incubated for 3 h at 37 °C. Headspace gas samples (60 μL) were injected into Agilent 8860 GC with a Restek column (ShinCarbon ST 80/100, 2 m, 1/8" OD) to analyze N₂O. These experiments were carried out in triplicate for each concentration of interest and three injections were performed for each vial.

Organ bath pharmacology: Mice (C57/BL6; wild type, WT) or soluble guanylyl cyclase knockout (sGC KO; kind gift of Michael Tones, Pfizer; male & female; 20–30 g) were euthanized by cervical dislocation. The thoracic aorta was carefully removed, cleaned of connective tissue and cut into three or four ring segments of approximately 4 mm in length. Aortic rings were mounted in 7 mL organ baths (Danish Myotechnology, Aarhus, Denmark) containing Krebs-bicarbonate buffer (composition (mM): Na⁺ 143; K⁺ 5.9; Ca²⁺ 2.5; Mg²⁺ 1.2; Cl⁻ 128; HCO₃⁻ 25; HPO₄²⁻ 1.2; SO₄²⁻ 1.2; d-Glucose 11) and gassed with carbogen (95% O₂/5% CO₂; British Oxygen Company; BOC; Guildford, UK). Tension was initially set at 0.3 g and reset at intervals following an equilibration period of approximately 1 h during which time fresh Krebs-bicarbonate buffer was replaced every 15 min. After equilibration, the rings were primed with three separate additions of KCl (48 mM; Sigma Aldrich, Poole, UK), at each addition maximum tension was observed (approx. 3 min) before being washed out by the addition of fresh Krebs-bicarbonate buffer at 10 min intervals for a total of 30 min. Cumulative concentrations of the α-adrenoceptor agonist phenylephrine (PE; 1 nM–3 μM) were then added until a maximum contraction was observed. Another washout period was performed before vessels were contracted to an EC₅₀ concentration of PE. Once this response had stabilized, a single addition of the endothelium-dependent dilator acetylcholine (ACh; 1 μM) was added to the bath to assess the integrity of the endothelium. If the contractions to PE were not maintained, or ACh produced

relaxations of less than 50% of the PE-tone, tissues were discarded (apart from denuded studies; see below).

After another wash period, the vessels were again contracted with PE (EC₈₀) and cumulative concentration response curves to S-nitroso-*N*-acetyl-penicillamine (SNAP; 1 nM–10 μM), CysSSCys (100 nM–300 μM), or RSSH donor **1** (100 nM–300 μM) were constructed. Tone was raised to the same PE EC₈₀ as that determined in the absence of L-NAME/ODQ/endothelial denudation or in WT tissues (for SGC KO). Responses to SNAP were also studied in the presence of CysSSCys and **1** (both at 10 μM; 15 min pre-incubation). In turn, concentration-dependent responses to CysSSCys and **1** (100 nM–300 μM) were explored in the presence of SNAP (100 μM; 30 min pre-incubation and washout). In further studies, to establish the NO-dependency of vasorelaxant responses to CysSSCys, concentration-dependent relaxations to CysSSCys were evaluated in the presence of the NO synthase inhibitor N^G-nitro-L-arginine methyl-ester (L-NAME; 300 μM; 15 min pre-incubation), the soluble guanylyl cyclase (sGC) inhibitor 1H-[1,2,4]oxadiazolo [4,3-*a*]quinoxalin-1-one (ODQ) (5 μM), following denudation of the endothelium (rubbing gently the internal surface of each aortic ring with forceps and determined by a lack [<10%] relaxation to ACh [1 μM]), or in tissues from SGC knockout mice.

Acute blood pressure measurement in anaesthetized mice: Mice (C57/BL6; WT; male and female; 20–30 g) were anaesthetized with 1.5% isoflurane (Abbott Laboratories Ltd, Queenborough, UK) in O₂ and placed supine on a thermostatically controlled heating blanket (37.0 °C ± 0.5 °C). To measure blood pressure, the left common carotid artery was isolated and a fluid-filled (heparin; 100U/ml diluted in 0.9% saline), 0.28 mm internal diameter cannula (Critchley Electrical Products Pty Ltd, Castle Hill, Australia) introduced into the artery. Blood pressure was measured using an in-line P23 XL transducer (Viggo-Spectramed, USA, California) and PowerLab system, calibrated beforehand, and recorded using LabChart (ADInstruments, Castle Hill, Australia). The jugular vein was cannulated for drug administration. The arterial cannula was flushed once with heparinized saline (heparin; 100 U/ml diluted in 0.9% saline). After a minimum 10 min equilibration or until continuous stable pressure was observed, mice were given an intravenous bolus injection of CysSSCys (1–10 mg/kg), **1** (1–10 mg/kg) or sodium nitroprusside (SNP; 1–10 μg/kg).

Computational Studies: Density functional theory (DFT) calculations were carried out using Gaussian 16 [18] at the SMD(H₂O)-M06-2X/def2-SVP//M06-2X/def2-SVP level of theory (see SI for details) [19–23]. Intrinsic reaction coordinate (IRC) calculations were performed to confirm the transition state structures (TSSs) connect the expected minima [24–26]. The robustness of our chosen level of theory was investigated through a benchmark study with other functionals, basis sets and solvents (see SI for details); our mechanistic conclusions persist independent of the method used. All computed structures and coordinates can be found at the ioChem-BD repository [27] at the following DOI: <https://doi.org/10.19061/iochem-bd-6-130>.

3. Results

Generation of NO (and other species) from the RSSH/RS-NO reaction: As has been proposed and reported previously, the reaction of RSSH with RS-NO can lead to the formation of RSSSR and NO [12] and **Reactions 1–3** have been proposed to explain these results. In this previous work, it was not determined whether other products aside from NO could also be generated. For example, although **Reactions 1–3** can account for R'S-NO degradation and NO liberation, it must be realized that this is not the only potential reaction pathway. Aside from the transnitrosation pathway (i.e., the transfer of the nitrosonium ion from one sulfur to another), whereby nucleophilic attack occurs at the nitrogen atom of R'S-NO, it is also known that nucleophilic attack can occur at the sulfur atom of R'S-NO [e.g., [28]. This reaction is referred to as an S-thiolation. If the nucleophile is RSSH/RSS[–], then the products would be nitroxyl (HNO) and the corresponding dialkyltrisulfide

(RSSSR[–]) **Reaction 4.**



Direct analysis of HNO formation is often problematic due to rapid dimerization to give, eventually, nitrous oxide (N₂O) (**Reaction 5**) [e.g., [29]



Indeed, due to **Reaction 5**, the detection of N₂O can be used as an indication of the intermediacy of HNO in a chemical system [e.g., [30]. Thus, membrane inlet mass spectrometry (MIMS) is used to monitor the generation of NO, N₂O and other volatile, neutral species from the reaction of an S-nitrosothiol and an RSSH species. Due to self-reactivity, hydopersulfides are inherently unstable and typically examined using persulfide donors [e.g., [31,32,33]. Therefore, these studies are performed using an alkylamine-substituted perthiocarbamate persulfide donor **1** (Fig. 1) [15] and S-nitrosoglutathione (GSNO) as the representative RS-NO species. As shown in Fig. 1, RSS[–] generated from the decomposition of **1** can have several possible fates in the presence of GS-NO; pathway A leads to NO formation and pathway B results in the eventual formation of N₂O (i.e., via the intermediacy of HNO). The RSSH donor **1** has a half-life of 16.7 min in aqueous solution at pH 7.4 and 37 °C and in the absence of any other reactant, an RSSH species formed from the breakdown of **1** will react with another unreacted molecule of **1** to give the corresponding dialkyltrisulfide and a thiocarbamate intermediate, which subsequently decomposes to produce carbonyl sulfide (COS) [15] (Fig. 1, pathway C). Thus, the generation of NO, N₂O and/or COS provide qualitative evidence for the existence/prevalence of the various pathways depicted in Fig. 1.

MIMS analysis of reaction mixtures containing 100 μM GSNO and increasing concentrations of **1** (50, 100 and 200 μM) was carried out in pH 7.4 buffer, in the dark and at 37 °C shows NO generation, indicating that pathway A appears to predominate under all reaction conditions (Fig. 2a–c). Not unexpectedly, the level of COS increase with increasing concentrations of **1** since the higher levels of **1** allow the COS forming pathway to compete (Fig. 1, pathway C). A qualitative assessment of the amount of N₂O generated from these reactions was carried out via GC headspace analysis and comparison to a standard curve generated from Angeli's salt decomposition (i.e., Angeli's salt is an established and reliable HNO donor [34]) (Fig. 2d). Based on this analysis, the yield of N₂O was approximately 13–20%, which represents approximately 26–40% of the total possible nitrogen containing products (i.e., two HNO molecules dimerize to generate one N₂O, **Reaction 5**). To be sure, extrapolation of HNO generation by pathway B (Fig. 1) from these reactions via the measurement of N₂O is apt to be artificially high since N₂O can also be generated in this system by the reaction of HNO with two molecules of NO (**Reaction 6**) [e.g., [35]. Thus, this reaction can result in a higher apparent yield of HNO (via N₂O measurement) and an artificially low apparent yield of NO from this chemistry.



Importantly, no H₂S was observed in these analyses (data not shown), indicating the absence of RSSH disproportionation chemistry (*vide infra*).

For comparison, the reaction of a structurally analogous thiol, *N*-acetylpenicillamine methyl ester (the thiol (RS[–]/RSH) analog of RSS[–] in Fig. 1) with GSNO was also examined. Comparison of the results shown in Fig. 2 (with RSSH + GSNO) with those of Fig. 3 (RSH + GSNO) shows clear qualitative differences between the levels of NO released under these two conditions (e.g., compare the magnitudes of the y-axes). It is clear that RSS[–]/RSSH is far superior to RS[–]/RSH in generating NO from reaction with RS-NO. This is especially evident when considering that the formation of RSS[–]/RSSH occurs slowly (*t*_{1/2} = 16.7 min [15]) under the conditions of these experiments due to generation via a donor species while the levels of RS[–]/RSH are present from the beginning at the

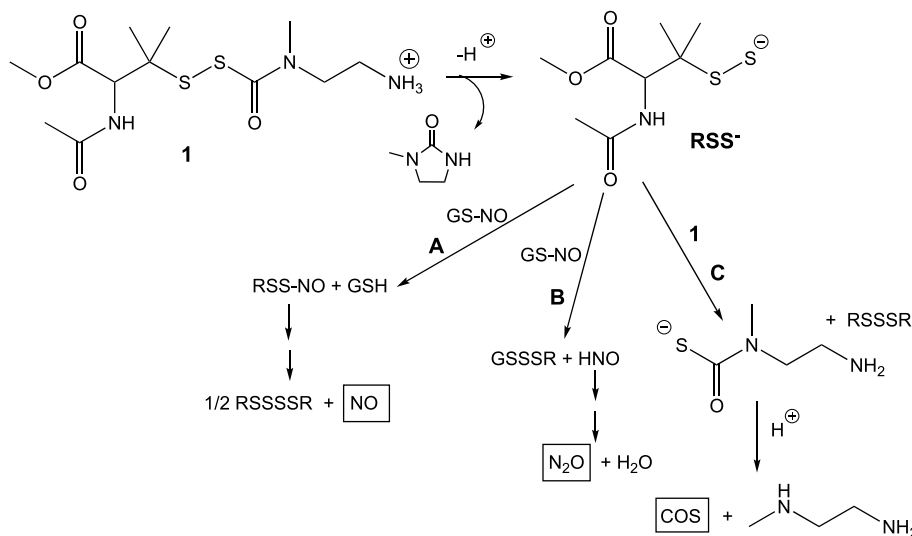


Fig. 1. Possible pathways for the reaction between **1** and GS-NO. Pathway A: Transnitrosation between RSS[−] and GS-NO and subsequent generation of NO. Pathway B: S-Thiolation of GS-NO by RSS[−] and generation of HNO. Pathway C: RSS[−] Reaction with excess **1**, leading to the eventual generation of COS.

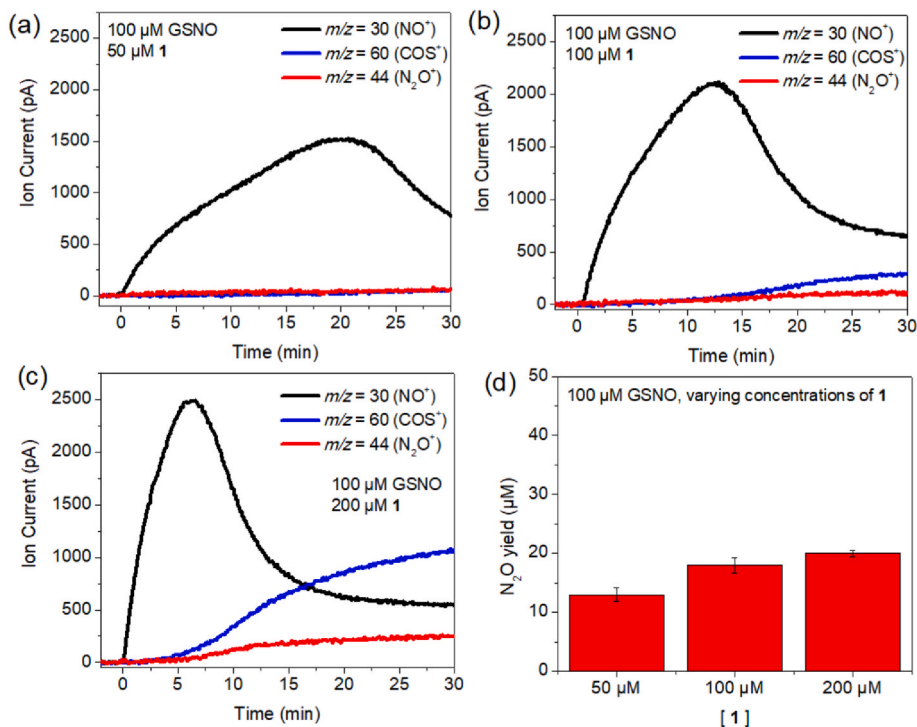


Fig. 2. MIMS signals observed during the incubation of GSNO (100 μ M) with (a) 50 μ M, (b) 100 μ M and (c) 200 μ M of RSSH donor **1**. $m/z = 30$ corresponds to NO^+ , $m/z = 60$ corresponds to COS^+ , and $m/z = 44$ corresponds to N_2O^+ . (d) N_2O yields independently quantified via GC headspace analysis (\pm SD). All reactions were carried out under anaerobic conditions in PBS (pH 7.4, 100 mM) containing diethylenetriaminepentaacetic acid (DTPA) (100 μ M) at 37 °C and protected from light.

stated concentrations. In addition, under these reaction conditions, N_2O is not observed by GC headspace analysis, consistent with the MIMS data.

Computational analysis of the RSSH/RS-NO reaction: To gain further insight into the reaction of RSSH with R'S-NO, a series of computational studies were performed at the SMD(H₂O)-M06-2X/def2-SVP//M06-2X/def2-SVP level. The deprotonation of RSSH followed by attack of the nucleophile RSS[−] on the nitrogen of R'S-NO yields the formation of an S-nitrosopersulfide intermediate (RSS-NO). This reaction is predicted to be endergonic by 4.2 kcal/mol and is reversible which can be attributed to RSS[−] being a better nucleophile compared to RS[−] due to a mild α -effect

[e.g., [31]. RSS-NO is kinetically and thermodynamically unstable at room temperature (S–N bond length is 1.9 \AA , BDE = approx. 4 kcal/mol [12]) and thus, it readily dissociates into perthiyl radical (RSS[−]) and nitric oxide (NO). The relatively stable RSS[−] species are non-oxidizing in contrast to their RS[−] counterparts due to delocalization of the odd electron [e.g., [12–14,31], but can dimerize to form dialkyltetrasulfide (RSSSSR) which is predicted to be exergonic by ~20 kcal/mol (Fig. 1, and Fig. 4, pathway A).

As discussed previously, there is an alternative pathway for these reactants. Pathway B (Fig. 1) generates HNO instead of NO via RSSH attack on the sulfur of R'S-NO to form RSSSR' and HNO [28]. This

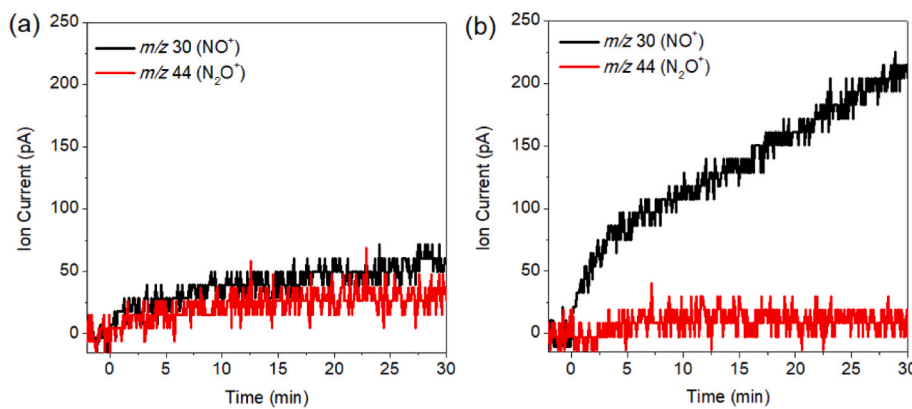


Fig. 3. MIMS analysis of the reaction of 100 μM GSNO with *N*-acetyl penicillamine methyl ester at (a) 50 μM and (b) 200 μM . Reaction carried out under same conditions as described for the experiments shown in Fig. 2.

S-thiolation reaction involves a proton transfer from RSSH to the nitrogen of R'S-NO followed by an asynchronous event of S-S bond formation and HNO liberation. (A proton transfer to the nitrogen of R'S-NO is more favorable than a proton transfer to the oxygen of R'S-NO. See SI for details.) The barrier for the formation of RSSSR and HNO is quite high and predicted to be 52.4 kcal/mol with respect to the sum of separate reactant energies. However, the energy profile of the S-thiolation reaction shown in Fig. 4 (pathway b) indicates that the bulk of the barrier is due to the proton transfer event, which is unfavorable without an explicit polar solvent (or enzymatic) environment; note that from the second structure shown, where the proton has largely transferred to nitrogen, the remaining barrier is only \sim 10 kcal/mol (We incorporated continuum water and chloroform via single point energy calculations. See SI for details). Thus, if the *N*-protonated R'S-NO and RSS $^{\cdot}$ are readily available, the S-thiolation step would be highly favorable with a small barrier at most.

The S-thiolation with simple thiols (RSH) has been previously studied by Timerghazin and co-workers who found a similar reaction path [36]. To compare the role of RSSH versus RSH in the reaction, we reproduced their S-thiolation analysis (Fig. 5, top) (Energies differ slightly from Timerghazin's energies due to the difference in the choice of level of theory.) The energy profile for the HNO generating reaction shows a high barrier as expected since it again includes the energy needed for the proton transfer (Fig. 5, bottom). The electronic energy (M06-2X/def2-SVP) barrier for the S-thiolation reaction after the proton transfer is 3.6 kcal/mol. Hence, once the proton of RSSH or RSH species is transferred to the nitrogen of RS-NO, the HNO generation reaction becomes viable. However, inspection of the reaction pathways indicates that the barrier remaining after proton transfer is less for the system with two sulfurs, although both are small.

Vasorelaxation resulting from the RSSH/RS-NO reaction: As an extremely potent vasorelaxant, the presence of NO can be readily detected using a vascular tissue bath assay. Thus, if the RSSH/RS-NO reaction liberates NO, this should result in the relaxation of vascular tissue. In order to test this idea, the effect of vascular tissue pre-treatment with the nitrosonium (NO^+) donor *S*-nitroso-*N*-acetylpenicillamine (SNAP), which will transnitrosate cellular thiols resulting in cellular RSNO species [37], on persulfide-mediated vasorelaxation was examined. As shown in Fig. 6, the persulfide donors cysteine trisulfide (CysSSSCys, an established donor of Cys-SSH in cells [38]) and RSSH donor 1 [15] both exhibited significantly increased vasorelaxant potency in murine aorta after pre-treatment with SNAP (30 min incubation followed by washout) (10 μM). Moreover, the concentration-dependent relaxations to SNAP were enhanced by pre-treatment with CysSSSCys and, to a lesser extent, by 1 (Fig. 6C, D).

Although modestly potent, both RSSH donors CysSSSCys and 1 alone (i.e., no SNAP pre-treatment) exhibited vasorelaxant properties (Fig. 6

A, B, control). This effect may be the result of liberation of NO from endogenous sources of intracellular R'SNO via reaction with RSSH. To this end, further studies were conducted with CysSSSCys to determine the mechanism(s) underpinning this inherent vasorelaxation activity. Interestingly, the vasorelaxant response to CysSSSCys was significantly inhibited in the presence of the NO synthase inhibitor *l*-nitroarginine methyl ester [39] (*l*-NAME, 300 μM ; Fig. 7 A) and by endothelial denudation (Fig. 7 B). In addition, the relaxant effects of CysSSSCys were significantly attenuated in the presence of the sGC inhibitor ODQ or in tissues from sGC knockout mice (Fig. 7C and D). These findings are consistent with the idea that CysSSSCys (via formation of RSSH) is able to liberate NO from endogenous 'stores' which in turn elicits vasorelaxation via an sGC/cGMP-dependent process.

In vivo hypotensive actions: In order to test the idea that RSSH species may facilitate vasodilation (possibly via an RSSH/R'SNO interaction) in an *in vivo* model, CysSSSCys and 1, along with the established and clinically relevant NO-donor sodium nitroprusside (SNP), were administered to anaesthetized mice and blood pressure monitored. All treatments produced a dose-dependent reduction in mean arterial blood pressure (MABP; Fig. 8). The potency of the NO donor was approximately three orders of magnitude greater than either persulfide donor.

4. Discussion

Herein, it is confirmed that RSSH has a great potential to react with R'S-NO species. This is not surprising since the electrophilic R'S-NO readily transnitrosates with nucleophilic RS $^{\cdot}$ /RSH species (although this is not a particularly fast reaction, $k = 5 - 170 \text{ M}^{-1}\text{s}^{-1}$, depending on the nature of the reactants [37]) (Reaction 7) and RSSH is a far superior nucleophile compared to RSH.



Previous work by Timerghazin and co-workers [36] on the RSH/R'SNO transnitrosation/S-thiolation reactions indicates that a competing S-thiolation reaction (Reaction 8) can also occur but is heavily dependent on a proton transfer event (or proper protonation states of the reactants) to facilitate reaction at sulfur (instead of at nitrogen as is the case for transnitrosation).



That is, the S-thiolation reaction is disfavored versus transnitrosation without specific catalysis or conditions that would facilitate protonation on the RS-NO nitrogen (to increase electrophilicity of the sulfur atom) and deprotonation of RSH (to increase nucleophilicity). Without these specific protonation-deprotonation events, S-thiolation and, therefore, HNO generation from this reaction is not favored.

In the analogous reaction to the RSH/R'S-NO reaction described

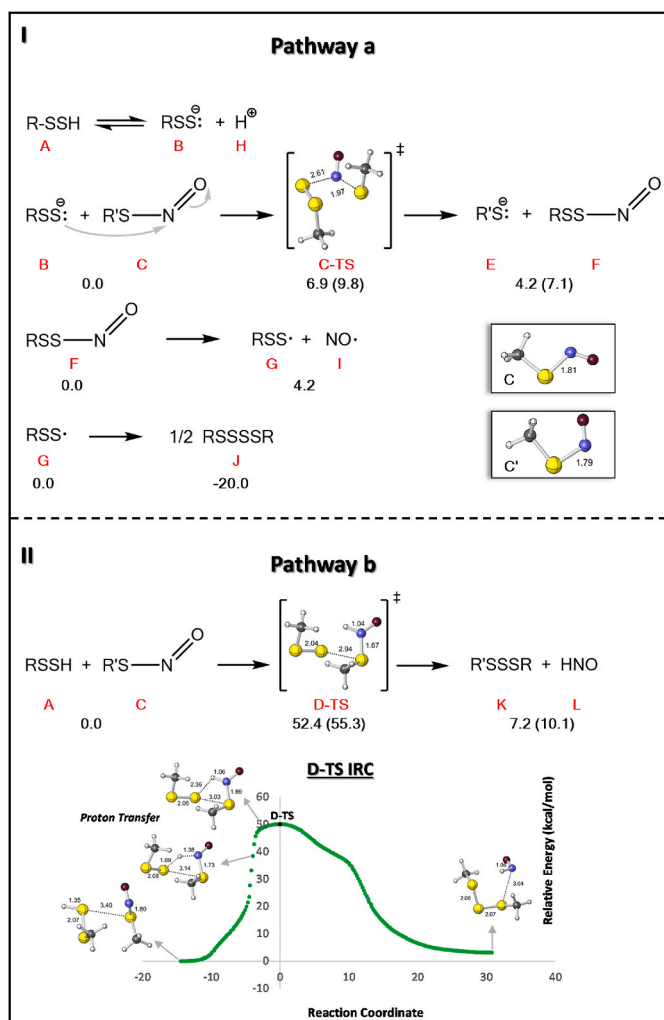


Fig. 4. I. Computed ($[SMD\text{-H}_2\text{O}]\text{-M06-2X/def2-SVP//M06-2X/def2-SVP}$) relative free energies (kcal/mol) for minima and TSSs involved in pathway a. There are two conformers of C (C and C'). Energies in the parenthesis are relative to the sum of the energies of C' and B, whereas the energies without the parenthesis are relative to the sum of the energies of C and B. II. On top: Computed ($[SMD\text{-H}_2\text{O}]\text{-M06-2X/def2-SVP//M06-2X/def2-SVP}$) relative free energies (kcal/mol) for minima and TSSs involved in pathway b. There are two conformers of C (C and C'). Energies in the parenthesis are relative to the sum of the energies of C' and A, whereas the energies without the parenthesis are relative to the sum of the energies of C and A. At the bottom: The electronic energy profile of the D'-TS (M06-2X/def2-SVP). The D'-TS is located where $x = 0$ on the plot. The electronic energy at each point in the IRC is relative to the electronic energy of the reactant complex (kcal/mol). The electronic energy barrier after the proton transfer is 0.5 kcal/mol. The bond distances are in Å. ($R = R' = \text{CH}_3$).

immediately above, the RSSH/R'S-NO reaction can also follow two pathways: transnitrosation (pathway A, Fig. 1) and S-thiolation (pathway B, Fig. 1). Unlike transnitrosation in the RSH/R'S-NO reaction (which simply produces another RS-NO species and is readily reversible), the RSSH/R'S-NO transnitrosation reaction generates a distinct and fleeting intermediate, RSS-NO, which can spontaneously homolyze to give NO and the perthiyl radical, RSS[·] (**Reaction 2**). Under purely chemical conditions, dimerization of RSS[·] occurs to generate RSSSSR [12,13,14] and thus this process can be considered to be essentially irreversible. Experimental results analyzing the small molecule products of the RSSH/R'S-NO reaction show a predominance of NO formed with lesser amounts of HNO (as measured by N_2O formation), (Fig. 2). As mentioned previously, HNO generation is undoubtedly overestimated in

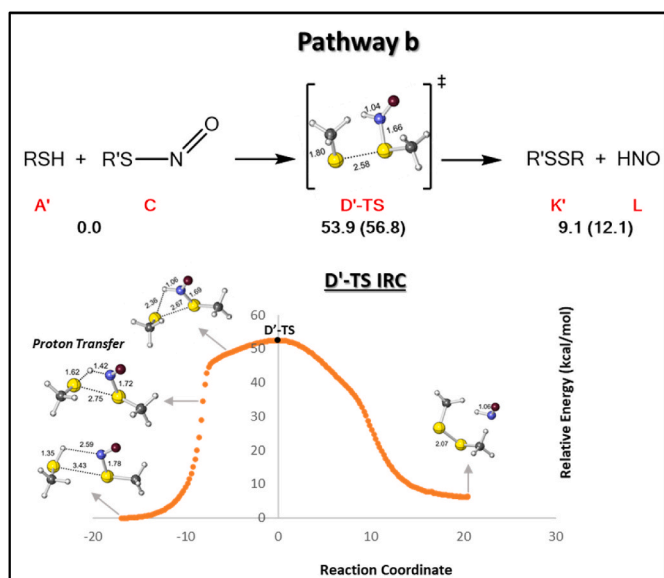


Fig. 5. On top: Computed ($[SMD\text{-H}_2\text{O}]\text{-M06-2X/def2-SVP//M06-2X/def2-SVP}$) relative free energies (kcal/mol) for minima and TSSs involved in pathway b. There are two conformers of C (C and C'). Energies in the parenthesis are relative to the sum of the energies of C' and A', whereas the energies without the parenthesis are relative to the sum of the energies of C and A'. At the bottom: The electronic energy profile of the D'-TS (M06-2X/def2-SVP). The D'-TS is located where $x = 0$ on the plot. The electronic energy at each point in the IRC is relative to the electronic energy of the reactant complex (kcal/mol). The electronic energy barrier after the proton transfer is 0.5 kcal/mol. The bond distances are in Å. ($R = R' = \text{CH}_3$).

these experiments due to alternative pathways for N_2O formation besides simple HNO dimerization (e.g., **Reaction 6**). This result is consistent with the idea that transnitrosation between R'S-NO and RSSH not only occurs readily, but also results in the generation of free NO. Importantly, a comparison of RSH and RSSH reaction with R'S-NO shows significantly less (approximately 10–30 fold) NO generated (comparing the results of Fig. 2a,c and 3a,b). Also, it should be stressed that in these experiments RSSH is generated using a donor species with a $t_{1/2}$ of approximately 16.7 min under the conditions of these experiments. Thus, the levels of RSSH build up over time and will never be as high as the stated concentrations of the donor. However, in the experiments using RSH, the thiol exists at the stated initial concentration. Thus, in the comparison of NO formation from the RSH/R'S-NO versus RSSH/R'S-NO reactions, the NO-forming capacity of the RSSH/R'S-NO reaction is likely to be significantly greater than the 10–30 fold differences observed in these experiments.

Computational analysis of the RSSH/R'S-NO reaction also indicates a favored transnitrosation reaction, leading to NO generation (Fig. 1 pathway a), as opposed to an S-thiolation reaction, that leads to HNO formation (Fig. 1, pathway b). However, it is also determined that the HNO-forming S-thiolation reaction with RSSH is more favorable than the HNO-forming S-thiolation reaction with RSH. The primary impedance for S-thiolation for the RSSH/R'S-NO reaction is the unfavorable and requisite proton transfer event (or the requirement for specific protonation on the nitrogen of R'S-NO and the deprotonation of the attacking RSSH). This result is entirely consistent with the results previously reported by Timerghazin et al. [36] for the RSH/R'S-NO reaction. It should be stressed, however, that the relative favorability of these reactions will be highly dependent on the pH, reactant ratios, sterics and specific protonation events (e.g., that may occur within specific protein environments). Thus, in a biological milieu or at specific protein sites, either pathway may be viable (albeit all things being equal, the transnitrosation pathway appears favorable).

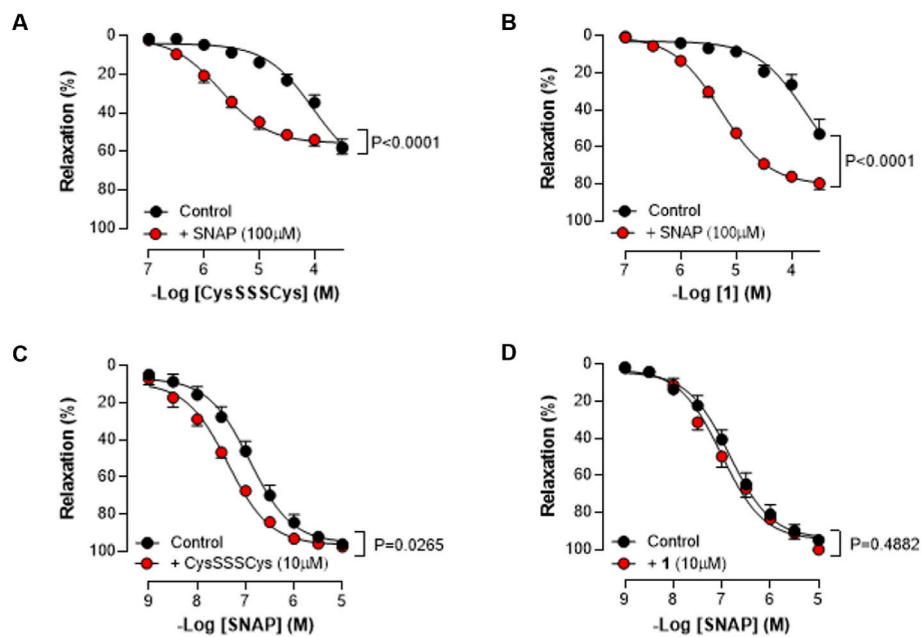


Fig. 6. Concentration-response curves to CysSSCys (A) or RSSH donor 1 (B) in the absence and presence of SNAP (100 μ M). Concentration-response curves to SNAP (C, D) in the absence and presence of CysSSCys (10 μ M; C) or 1 (10 μ M; D). Data are expressed as mean \pm sem with statistical analysis conducted by two-way analysis of variance. n = 8.

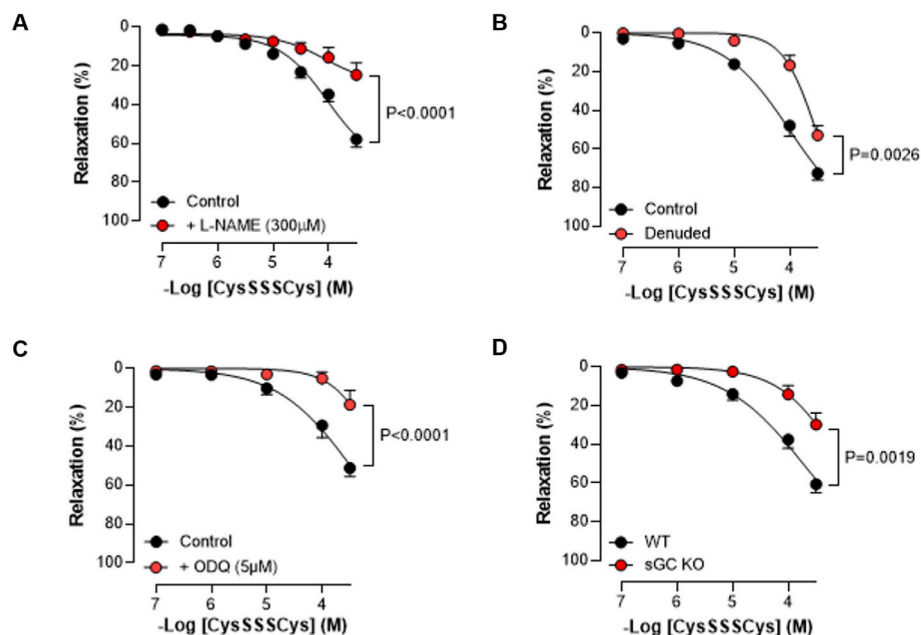


Fig. 7. Concentration-response curves to CysSSCys in the absence and presence of the NO synthase inhibitor L-NAME (300 μ M; A), endothelial denudation (B), the sGC inhibitor ODQ (5 μ M; C) or in wild type (WT) and sGC knockout (KO) mice (D). Data are expressed as mean \pm sem with statistical analysis conducted by two-way analysis of variance. n = 8.

As stated earlier, R'S-NO species have been proposed to be storage forms and/or reservoirs of NO that can be liberated to, for example, control vascular tone [e.g., [40,41]]. In the case of possible NO liberation from an S-nitrosothiol on hemoglobin, a novel electron transfer from a deoxygenated ferrous heme to the S-nitrosothiol function has been proposed as a possible mechanism of NO liberation [42,43]. However, in cases where this possibility does not exist (i.e., in cases lacking a nearby ferrous iron), reasonable mechanisms for NO liberation from RS-NO remain unestablished. Herein using vasorelaxation as a biologically relevant and specific detector of NO, it is shown that smooth muscle

tissues pre-loaded with R'S-NO (via pre-treatment with the S-nitrosothiol SNAP) exhibit a marked increase in RSSH-mediated vasorelaxation (Fig. 6 A, B); likewise, the vasorelaxant activity of SNAP is enhanced by RSSH pretreatment (Fig. 6C, D). These observations support a mechanism dependent on NO release via **Reactions 1, 2**. This concept was confirmed by establishing that the vasorelaxant actions of RSSH were blocked in the presence of sGC inhibition (with ODQ) and in tissues from sGC KO mice (Fig. 7C, D). Importantly, in vascular tissue that is not pre-treated with an S-nitrosothiol, RSSH still has vasorelaxant properties, albeit with a much decreased potency compared to R'S-NO

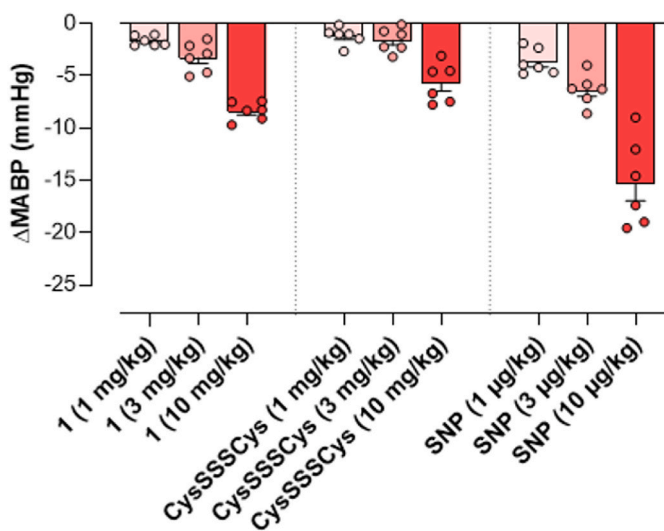


Fig. 8. Dose-dependent reductions in mean arterial blood pressure (MABP) in response to bolus, intravenous administration of **1**, CysSSCys and sodium nitroprusside (SNP). $n = 8$.

pretreated tissues. Interestingly, the vasorelaxant properties of RSSH are markedly diminished in the presence of an NOS inhibitor and following endothelial denudation (Fig. 7 A, B), implicating endogenous NO biosynthesis in at least some of the vasorelaxant effects associated RSSH. At this time, this effect is not fully understood. However, it can be speculated that some portion of NOS-derived NO results in R'S-NO formation (thereby intimating a dynamic endogenous synthetic pathway) and therefore inhibition of NOS decreases R'S-NO and therefore, diminishes the effect of exogenous RSSH. It is important to note that the vasorelaxant properties of S-nitrosocysteine can be enhanced by the presence of Cys-SH [44]. However, our chemical studies comparing the ability of RSH and RSSH to release NO via reaction with R'S-NO would predict that RSSH would be much more potent in this regard (compare Fig. 2a with Fig. 3a). Regardless, this study presents the possibility that RSSH species are capable of degrading R'S-NO in biological tissues with subsequent liberation of NO, as indicated by a vasorelaxant response. Furthermore, consistent with the idea that RSSH can serve to liberate NO from endogenous R'S-NO sources, leading to vasorelaxation, RSSH species are shown to possess vasorelaxant properties *in vivo* in anaesthetized mice (Fig. 8).

R'S-NO species have also been proposed to be deleterious. For example, aberrant overproduction of NO, leading to excessive R'S-NO formation in critical proteins has been implicated in the etiology of neurodegenerative disease [5] and cancer [6]. As such, processes that regulate steady-state R'S-NO levels in cells become of considerable interest with regards to the development of possible disease therapies. As mentioned previously, RSSH are oxidized with respect to RSH and therefore may be expected to be more prevalent under oxidizing cellular conditions [e.g., 11]. As RSSH are superior nucleophiles and reductants compared to the corresponding RSH species, their biological generation presents the scenario that a superior reductant is generated primarily during oxidative stress conditions and therefore can serve a protective role. Importantly, this idea has experimental support from studies reporting protective actions of RSSH against oxidative and/or electrophilic stress [for example, 38,33,45–50]. Thus, R'S-NO species generated under oxidative stress conditions (consider that R'S-NO species are also oxidized with respect to RSH) may be particularly susceptible to destruction by the RSSH chemistry described herein. Thus, in this way, endogenous RSSH generation may serve to protect a cell from aberrant and potentially harmful R'S-NO formation. To be sure, R'S-NO species are also proposed as normal physiological signaling agents and even protectants against RSH overoxidation [e.g., 51]. Thus, the generation

of an R'S-NO reactive species, such as RSSH, may only be beneficial under conditions of an over-production and potentially deleterious levels of R'S-NO, such as may be the case under oxidative stress.

Funding

JPT acknowledges the National Science Foundation (CHE-1900285) for generous support for this research. C.P.T. and A.J.H. were supported by a British Heart Foundation Programme Grant (RG/16/7/32357).

Declaration of competing interest

The authors declare no conflicts of interest.

Acknowledgements

The authors thank NSF's XSEDE program for computational support. The authors also thank David Wink, Yoshito Kumagai and Taka Akaike for their helpful discussions.

Appendix A. Supplementary data

Supplementary data to this article can be found online at <https://doi.org/10.1016/j.freeradbiomed.2022.06.245>.

References

- [1] B.S. Rayner, B.-J. Wu, M. Raftery, R. Stocker, P.K. Wittig, Human S-nitroso Oxymyoglobin is a store of vasoactive nitric oxide, *J. Biol. Chem.* 280 (2005) 9985–9993.
- [2] D.J. Singel, J.S. Stamler, Chemical physiology of blood flow regulation by red blood cells: the role of nitric oxide and S-nitrosohemoglobin, *Annu. Rev. Physiol.* 67 (2005) 99–145.
- [3] L.J. Ignarro, H. Lipton, J.C. Edwards, W.H. Baricos, A.L. Hyman, P.J. Kadowitz, C. A. Gruetter, Mechanism of vascular smooth muscle relaxation by organic nitrates, nitrites, nitroprusside and nitric oxide: evidence for the involvement of S-nitrosothiols as active intermediates, *J. Pharmacol. Exp. Therapeut.* 218 (1981) 739–749.
- [4] T. Nakamura, O.A. Prikhodko, E. Pirie, S. Nagar, M.W. Akhtar, C.-K. Oh, S. R. McKercher, R. Ambasudhan, S. Okamoto, S.A. Lipton, Aberrant protein S-nitrosylation contributes to the pathophysiology of neurodegenerative diseases, *Neurobiol. Dis.* 84 (2015) 99–108.
- [5] T. Nakamura, S.A. Lipton, 'SNO'-storms compromise protein activity and mitochondrial metabolism in neurodegenerative disorders, *Trends Endocrinol. Metabol.* 28 (2017) 879–892.
- [6] P. Ehrenfeld, F. Cordova, W.N. Duran, F.A. Sanchez, S-nitrosylation and its role in breast cancer angiogenesis and metastasis, *Nitric Oxide* 87 (2019) 52–59.
- [7] S. Rizza, G. Filomeni, Exploiting S-nitrosylation for cancer therapy: facts and perspectives, *Biochem. J.* 477 (2020) 3649–3672.
- [8] J.M. Fukuto, C. Perez-Ternero, J. Zarenkiewicz, J. Lin, A.J. Hobbs, J.P. Toscano, Hydrosulfides (RSSH) and nitric oxide (NO) signaling: possible effects on S-nitrosothiols, *Antioxidants* 11 (2022) 169.
- [9] J.I. Toohey, A.J.L. Cooper, Thiosulfoxide (sulfane) sulfur: new chemistry and new regulatory roles in biology, *Molecules* 19 (2014) 12789–12813.
- [10] J.M. Fukuto, L.J. Ignarro, P. Nagy, D.A. Wink, C.G. Kevil, M. Feelisch, M. Cortese-Krott, C.L. Bianco, Y. Kumagai, A.J. Hobbs, J. Lin, T. Akaike, Biological hydrosulfides and related polysulfides: a new concept and perspective in redox biology, *FEBS Lett.* 592 (2018) 2140–2152.
- [11] J.M. Fukuto, A.J. Hobbs, A comparison of the chemical biology of hydrosulfides (RSSH) with other protective biological antioxidants and nucleophiles, *Nitric Oxide* 107 (2021) 46–57.
- [12] C.L. Bianco, T.A. Chavez, V. Sosa, S.S. Saund, Q.N.N. Nguyen, D.J. Tantillo, A. S. Ichimura, J.P. Toscano, J.M. Fukuto, The chemical biology of the persulfide (RSSH)/perthiyl (RSS-) redox couple and possible role in biological redox signaling, *Free Radic. Biol. Med.* 101 (2016) 20–31.
- [13] S.A. Everett, P. Wardman, Persulfides as antioxidants: radical-scavenging and prooxidative mechanisms, *Methods Enzymol.* 251 (1995) 55–69.
- [14] J.P.R. Chauvin, M. Griesser, D.A. Pratt, Hydrosulfides: H-atom transfer agents par excellence, *J. Am. Chem. Soc.* 39 (2017) 6484–6493.
- [15] V.S. Khodade, B.M. Pharoah, N. Paolocci, J.P. Toscano, Alkylamine-substituted perthiocarbamates: dual precursors to hydrosulfide and carbonyl sulfide with cardioprotective actions, *J. Am. Chem. Soc.* 142 (2020) 4309–4316.
- [16] T.A. Chavez, J.P. Toscano, in: M.A. Marti, F. Doctorovich, P. Farmer (Eds.), *Detection of HNO by Membrane Inlet Mass Spectrometry* in the *Chemistry And Biology of Azanone (HNO)*, Elsevier, 2017, pp. 255–267.
- [17] J. Zarenkiewicz, V.S. Khodade, J.P. Toscano, Reaction of nitroxyl (HNO) with hydrogen sulfide and hydrosulfides, *J. Org. Chem.* 86 (2021) 868–877.

[18] Gaussian 16, Revision A.03, M.J. Frisch, G.W. Trucks, H.B. Schlegel, G.E. Scuseria, M.A. Robb, J.R. Cheeseman, G. Scalmani, V. Barone, G.A. Petersson, H. Nakatsuji, X. Li, M. Caricato, A.V. Marenich, J. Bloino, B.G. Janesko, R. Gomperts, B. Mennucci, H.P. Hratchian, J.V. Ortiz, A.F. Izmaylov, J.L. Sonnenberg, D. Williams-Young, F. Ding, F. Lipparini, F. Egidi, J. Goings, B. Peng, A. Petrone, T. Henderson, D. Ranasinghe, V.G. Zakrzewski, J. Gao, N. Rega, G. Zheng, W. Liang, M. Hada, M. Ehara, K. Toyota, R. Fukuda, J. Hasegawa, M. Ishida, T. Nakajima, Y. Honda, O. Kitao, H. Nakai, T. Vreven, K. Throssell, J. A. Montgomery Jr., J.E. Peralta, F. Ogliaro, M.J. Bearpark, J.J. Heyd, E. N. Brothers, K.N. Kudin, V.N. Staroverov, T.A. Keith, R. Kobayashi, J. Normand, K. Raghavachari, A.P. Rendell, J.C. Burant, S.S. Iyengar, J. Tomasi, M. Cossi, J. M. Millam, M. Klene, C. Adamo, R. Cammi, J.W. Ochterski, R.L. Martin, K. Morokuma, O. Farkas, J.B. Foresman, D.J. Fox, Gaussian, Inc., Wallingford CT, 2016.

[19] A.V. Marenich, C.J. Carmer, D.G. Truhlar, Universal solvation model based on solute electron density and on a continuum model of the solvent defined by the bulk dielectric constant and atomic force tensions, *J. Phys. Chem. B* 113 (2009) 6378–6396.

[20] F. Weigend, R. Ahlrichs, Balanced basis sets of split valence, triple zeta valence and quadruple zeta valence quality of H to Rn: design and assessment of accuracy, *Physiol. Chem. Phys.* 7 (2005) 3297–3305.

[21] F. Weigend, Accurate Coulomb-fitting basis sets for H to Rn, *Phys. Chem. Phys. Chem.* 8 (2006) 1057–1065.

[22] Y. Zhao, D.G. Truhlar, Density functionals with broad applicability in chemistry, *Acc. Chem. Res.* 41 (2008) 157–167.

[23] N. Mardirossian, M. Head-Gordon, How accurate are the Minnesota density functionals for noncovalent interactions, isomerization energies, thermochemistry and barrier heights involving molecules composed of main-group elements? *J. Chem. Theor. Comput.* 12 (2016) 4303–4325.

[24] C. Gonzalez, H.B. Schlegel, Reaction path following in mass-weighted internal coordinates, *J. Phys. Chem.* 94 (14) (1990) 5523–5527.

[25] K. Fukui, The path of chemical reactions - the IRC approach, *Acc. Chem. Res.* 14 (1981) 363–368.

[26] S. Maeda, Y. Harabuchi, Y. Ono, T. Taketsugu, K. Morokuma, Intrinsic reaction coordinate: calculation, bifurcation, and automated search, *Int. J. Quant. Chem.* 115 (2015) 258–269.

[27] M. Alvarez-Moreno, C. de Graaf, N. Lopez, F. Maseras, J.M. Poblet, C. Bo, Managing the computational chemistry big data problem: the ioChem-BD platform, *J. Chem. Inf. Model.* 55 (2015) 95–103.

[28] P.S.-Y. Wong, J. Hyun, J.M. Fukuto, F.N. Shiroda, E.G. DeMaster, H.T. Nagasawa, The reaction between nitrosothiols and thiols: generation of nitroxyl (HNO) and subsequent chemistry, *Biochemistry* 37 (16) (1998) 5362–5371.

[29] F.C. Kohout, F.W. Lampe, On the role of the nitroxyl molecule in the reaction of hydrogen atoms with nitric oxide, *J. Am. Chem. Soc.* 87 (1965) 5795–5796.

[30] F.T. Bonner, B. Ravid, Thermal decomposition of oxyhyponitrite (sodium trioxodinitrite(II)) in aqueous solution, *Inorg. Chem.* 14 (1974) 558–563.

[31] K. Ono, T. Akaike, T. Sawa, Y. Kumagai, D.A. Wink, D.J. Tantillo, A.J. Hobbs, P. Nagy, M. Xian, J. Lin, J.M. Fukuto, The redox chemistry and chemical biology of H₂S, hydrosulfides and derived species: implications of their possible biological activity and utility, *Free Radic. Biol. Med.* 77 (2014) 82–94.

[32] K.M. Dillon, J.B. Matson, A review of chemical tools for studying small molecule persulfides: detection and delivery, *ACS Chem. Biol.* 16 (2021) 1128.

[33] V.S. Khodade, S.C. Aggarwal, A. Eremiev, E. Bao, S. Porche, J.P. Toscano, Development of hydrosulfide donors to study their chemical biology, *Antioxid. Redox Signaling* 36 (2021) 309–326.

[34] S.B. King, H.T. Nagasawa, Chemical approaches toward generation of nitroxyl, *Methods Enzymol.* 301 (1999) 211–220.

[35] K.M. Miranda, The chemistry of nitroxyl (HNO) and implications in biology, *Coord. Chem. Rev.* 249 (2005) 433–455.

[36] L.V. Ivanova, D. Cibich, G. Deye, M.R. Talipov, Q.K. Timerghazin, Modeling of S-nitrosothiol-thiol reactions of biological significance: HNO production by S-thiolation requires a proton shuttle and stabilization of polar intermediates, *ChemBiochem* 18 (2017) 726–736.

[37] N. Hogg, The kinetics of S-transnitrosation – a reversible second-order reaction, *Anal. Biochem.* 272 (1999) 257–262.

[38] C.L. Bianco, T. Akaike, T. Ida, P. Nagy, V. Bogdandi, J.P. Toscano, Y. Kumagai, C. F. Henderson, R.N. Goddu, J. Lin, J.M. Fukuto, The reaction of hydrogen sulfide with disulfides: formation of a stable trisulfide and implications for biological systems, *Br. J. Pharmacol.* 176 (2019) 671–683.

[39] J.M. Fukuto, G. Chaudhuri, Inhibition of constitutive and inducible nitric oxide synthase: potential selective inhibition, *Annu. Rev. Pharmacol. Toxicol.* 35 (1995) 165–194.

[40] E.S.M. Ng, P. Kubes, The physiology of S-nitrosothiols: carrier molecules for nitric oxide, *Can. J. Physiol. Pharmacol.* 81 (2003) 759–764.

[41] J. Rodriguez, R.E. Maloney, T. Rassaf, N.S. Bryan, M. Feelisch, Chemical nature of nitric oxide storage forms in rat vascular tissue, *Proc. Natl. Acad. Sci. U.S.A.* 100 (2003) 336–341.

[42] J.P. Pezacki, N.J. Ship, R. Kluger, Release of nitric oxide from S-nitrosohemoglobin. Electron transfer as a response to deoxygenation, *J. Am. Chem. Soc.* 123 (2001) 4615–4616.

[43] N.J. Ship, J.P. Pezacki, R. Kluger, Rates of release of nitric oxide from HbSNO and internal electron transfer, *Bioorg. Chem.* 31 (2003) 3–10.

[44] M. Feelisch, M. te Poel, R. Zamora, A. Deussen, S. Moncada, Understanding the controversy over the identity of EDRF, *Nature* 368 (1994) 62–65.

[45] T. Ida, T. Sawa, H. Ihara, Y. Tsuchiya, Y. Watanabe, Y. Kumagai, M. Suematsu, H. Motohashi, S. Fujii, T. Matsunaga, M. Yamamoto, K. Ono, N.O. Devarie-Baez, M. Xian, J.M. Fukuto, T. Akaike, Reactive cysteine persulfides and S-polythiolation regulate oxidative stress and redox signaling, *Proc. Natl. Acad. Sci. USA* 111 (2014) 7606–7611.

[46] R. Greiner, Z. Palinkas, K. Basell, D. Becher, H. Antelmann, P. Nagy, T.P. Dick, Polysulfides link H₂S to protein thiol oxidation, *Antioxidants Redox Signal.* 19 (2013) 1749–1765.

[47] C.R. Powell, K.M. Dillon, Y. Wang, R.J. Carrazzone, J.B. Matson, A persulfide donor responsive to reactive oxygen species: insights into reactivity and therapeutic potential, *Angew. Chem. Int. Ed.* 57 (2018) 6324–6328.

[48] D. Ezerina, Y. Takano, K. Hanaoka, Y. Urano, T.P. Dick, N-Acetyl cysteine functions as a fast-acting antioxidant by triggering intracellular H₂S and sulfane sulfur production, *Cell. Chem. Biol.* 25 (2018) 1–13.

[49] T. Zhang, K. Ono, H. Tsutsuki, H. Ihara, W. Islam, T. Akaike, T. Sawa, Enhanced cellular polysulfides negatively regulate TLR4 signaling and mitigate lethal endotoxin shock, *Cell. Chem. Biol.* 26 (2019) 1–13.

[50] Henderson, C.F. Bica, I. Long, F.T. Irwin, D.D. Stull, C.H. Baker, B.W. Suarez-Vega, V. Taigher, Z.M. Fletes, E.D. Bartleson, J.M. Humphrey, M.L. Alvarez, L. Akiyama, M. Kumagai, T. Fukuto JM and Lin, J. Cysteine trisulfide protects *E. coli* from electrophile-induced death through the generation of cysteine hydrosulfide, *Chem. Res. Toxicol.*, 33, 678–686.

[51] J. Sun, C. Steenbergen, E. Murphy, S-nitrosylation: NO-related redox signaling to protect against oxidative stress, *Antioxidants Redox Signal.* 9&10 (2006) 1693–1705.